



## ***Kappa-Carrageenan Biopolymer-Based Nanocomposite Hydrogel and Adsorption of Methylene Blue Cationic Dye from Water***

**Gholam Reza Mahdavinia<sup>1</sup>, Ali Baghban<sup>2</sup>, Samira Zorofi<sup>2</sup>, Abdolhossein Massoudi<sup>2</sup>**

<sup>1</sup>Department of Chemistry, Faculty of Science, University of Maragheh, P.O. Box 55181-83111, Maragheh, Iran

<sup>2</sup>Department of Chemistry, Faculty of Science, Payame Noor University, P.O.Box19395-3697, Tehran, Iran

Received 22 Dec 2012, Revised 8 Nov 2013, Accepted 8 Nov 2013

\*Corresponding: [grmnia@maragheh.ac.ir](mailto:grmnia@maragheh.ac.ir), [gholamreza.mahdavinia@gmail.com](mailto:gholamreza.mahdavinia@gmail.com), Phone: +98-421-2273068, Fax: +98-421-227-3068

### **Abstract**

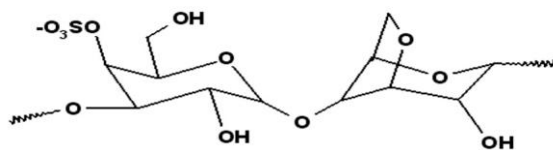
Nanocomposite hydrogels were synthesized by solution copolymerization of acrylamide (AAM) in the presence of *kappa*-carrageenan (Carra) biopolymer and sodium montmorillonite (Na-MMt) nanoclay. The structure and morphology of the nanocomposites were investigated using XRD and scanning electron microscopy (SEM). The obtained nanocomposites were examined to remove cationic methylene blue (MB) dye from water. The effect of clay content on the rate of dye adsorption revealed that the rate of dye adsorption enhanced by introduction of nanoclay in hydrogel composition. The results showed that the pseudo-second-order adsorption kinetic predominated for the adsorption of MB onto nanocomposites. The experimental equilibrated adsorption capacity of nanocomposites was analyzed using Freundlich and Langmuir isotherm models. The results corroborated that the experimental data fit the Langmuir isotherm the best.

**Keywords:** Carrageenan, Nanocomposite, Polyacrylamide, Hydrogel, Adsorption, Cationic Dye.

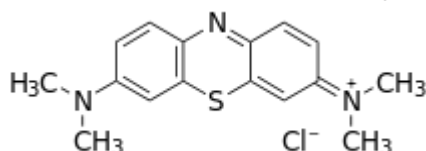
### **1. Introduction**

Hydrogels are type of three-dimensional hydrophilic polymers capable to swell and absorb a large amount of water [1]. They are mainly used in sanitary goods for absorbing the body fluids and in soil conditioning and improving the water retention capability of soil in agriculture and horticulture [2]. They are also found to be valuable in some specialized applications, including controlled delivery of bioactive agents [3] and wastewater treatment [4]. Hydrogels can be classified into non-ionic and ionic materials. The ionic types comprise anionic ( $-\text{CO}_2^-$ ,  $-\text{SO}_3^-$ ) or cationic pendants ( $-\text{NR}_3^+$ ) [5]. The presence of these ionic groups in the hydrogels opens potential area of application that is related to remove pollutants from wastewaters [6]. Industry is a huge source of water pollution; it produces pollutants that are excessively harmful to people and the environment. Colored water and solutions containing toxic heavy metals from many industries like dye, textile, paper, plastic, plating, and mining facilities produce considerable polluted waters. The pollutants must be removed from wastewater before discharge it into the environment. Adsorption process, an inexpensive and simple design, can be used to remove dye contaminants from aqueous environments [7]. The colors pollutants are anionic or cationic molecules. The existence of anionic and cationic pendants in the hydrogels makes them to show complexing ability with materials with opposite charges. So, anionic and cationic hydrogels have been used to remove anionic and cationic dyes from aqueous media [8, 9]. Similar to the dye removal, adsorption of heavy metal cations by anionic pendant of hydrogels is another capability of these materials [10]. But, these hydrogels mainly do not possess adequate strength. Introducing of nano-clays into hydrogels compositions can be considered as one of the methods to improve this property of hydrogels [11]. It has been reported that inclusion of nano-clays in the hydrogel composition can not only improve their strength but also the rate and dye adsorption capacity can be increased [12]. Nanocomposites hydrogels containing Na-montmorillonite [13], laponite [14], attapulgite [15], and sepiolite [16] have been synthesized and used to remove pollutants from aqueous media. Also, due to non-toxicity and biodegradability of biopolymers, the removal of dyes from water has been assessed by using nanocomposite hydrogels based on polysaccharides biomass [17].

Because of eco-friendly property of carrageenan with  $-\text{SO}_3^-$  groups (Scheme 1), we attempted to synthesize nanocomposite hydrogels by introduction of this biopolymer. In the previous works, we reported the adsorption of crystal violet cation dye onto nanocomposite hydrogels based on *kappa*-carrageenan from solution polymerization of acrylic acid monomer in the presence of Na-MMt and Laponite RD nanoclays [18-20]. The current work describes the synthesis of crosslinked polyacrylamide in the presence of carrageenan biopolymer and sodium montmorillonite nanoclay. The structures of nanocomposite hydrogels were investigated using XRD and SEM technique. The capability of the obtained nanocomposite hydrogels was examined to remove cationic methylene blue dye (Scheme 2) from water.



Scheme 1: Structure of kappa-carrageenan



Scheme 2: Structure of cationic methylene blue dye

## 2. Materials and methods

### 2.1. Materials

kappa-Carrageenan was obtained from Condinson Co., Denmark. N,N-methylenebisacrylamide (MBA) and ammonium persulfate (APS) from Fluka, and acrylamide from Rotterdam, the Netherlands, were of analytical grade and were used as received. Natural sodium-montmorillonite (sodium Cloisite, Na-MMT) as nanoclay with cation exchange capacity of 92 meq/100 g of clay was provided by Southern Clay Products. All other ingredients were analytical grades and were used as received.

### 2.2. Synthesis of Nanocomposite Hydrogels

Nanocomposite hydrogels based on kappa-carrageenan and crosslinked polyacrylamide were synthesized in the presence of Na-MMT nanoclay. The suffix *m* in Clay<sub>*m*</sub> is wt% of Clay in nanocomposite composition. In general, 0, 0.1, and 0.2 g of clay was dispersed in 30 mL of distilled water and stirred under magnetic stirrer for 24 h. Dispersed clay solution was transferred in a one-liter reactor equipped with mechanical stirrer. To control the reaction temperature, the reactor was placed in a water bath preset at 60 °C. Then, 0.5 g of kappa-carrageenan was added to the solution containing clay and stirred for 2 h until completion of dissolution. 3 g AAm and 0.05 g MBA (MBA dissolved in 3 mL of water) were simultaneously added into solution and allowed to stir for 1 h. Finally, APS (0.05 g in 2 mL of water) as initiator was added into solution and stirred for 3 min. The resultant nanocomposite hydrogels were cooled to ambient temperature and dried for 7 days. After this time, the dried nanocomposite hydrogels were grinded and kept from light and moisture.

### 2.3. Dye Adsorption Measurements

Dye adsorption was carried out by immersing the 0.05 g of nanocomposites into 50 mL of dye solution with 50 mg/L of MB solution. All adsorption experiments were examined through a batch method on a stirrer with a constant speed at 120 rpm. To study the adsorption kinetics, at specified time intervals, the amount of adsorbed MB was evaluated using a UV spectrometer at  $\lambda_{\max}=660$  nm. The content of adsorbed dye was calculated using following Eq 1:

$$q_t = \frac{(C_0 - C_t)}{m} \times V \quad (1)$$

where,  $C_0$  is the initial MB concentration (mg/L),  $C_t$  is the remaining dye concentrations in the solution at time  $t$ ,  $V$  is the volume of dye solution used (L), and  $m$  (g) is the weight of nanocomposite. Adsorption isotherm was carried out by immersing 0.05 g of nanocomposites into 50 mL of dye solutions with 10, 25, 50, 100, 200, 300, 500, 700, and 50 mg/L of MB for 24 h. The equilibrium adsorption capacity of nanocomposites,  $q_e$  (mg/g), was determined using Eq 1. At this Eq, the  $C_t$  and the  $q_t$  will be replaced with equilibrium concentration of dye in the solution ( $C_e$ ) and equilibrium adsorption capacity ( $q_e$ ), respectively.

### 2.4. Instrumental Analysis

For XRD and SEM studies, hydrogel nanocomposite containing 5 wt% of clay was synthesized in a glassy petri dish. Then, it cut into thin discs with diameter of approximately 10 mm. After purifying them by immersing in distilled water for 1 day, the discs were dried at ambient temperature. Dried nanocomposite was coated with a thin layer of gold and imaged in a SEM instrument (Vega, Tescan). One-dimensional, wide angle X-ray diffraction patterns were obtained by using a Siemens D-500 X-ray diffractometer with wavelength,  $\lambda=1.54\text{\AA}$  (Cu-K $\alpha$ ), at a tube voltage of 35 KV, and tube current of 30 mA.

## 3. Results and discussion

### 3.1. Synthesis and characterization

Semi-interpenetrating polymer network (Semi-IPN) nanocomposite hydrogels based on kappa-carrageenan were synthesized using solution polymerization. Na-MMT was used as nanoclay. Polymerization of AAm in the presence of

MBA produces network that kappa-carrageenan exists as linear biopolymer in this network. The XRD patterns of clay and nanocomposite were studied and shown in Figure 1. As shown in this figure, the XRD profile of pristine Na-MMt shows a diffractive peak at  $2\theta=7.6$  corresponding to the distance of clay sheets with  $d$  spacing  $11.61 \text{ \AA}$ . Stirring of clay for 24 h and subsequently in situ polymerization of AAm in the presence of MBA crosslinker leads to a nanocomposite hydrogel that the XRD profile of this hydrogel shown in Figure 1. No diffraction peak was observed in nanocomposite containing 5 wt% of clay (Clay0.2) and it can be concluded that the clay layers are exfoliated. One of the most important properties of nanocomposites which can be considered is hydrogel microstructure morphology. Figure 2 depicts surface morphology of hydrogel without clay (Figure 2a) and nanocomposite hydrogel (Figure 2b). While the hydrogels without clay shows a relatively smooth surface, the nanocomposite contains coarse and undulant surface. This observation can be attributed to insertion of nanoclay into hydrogel.

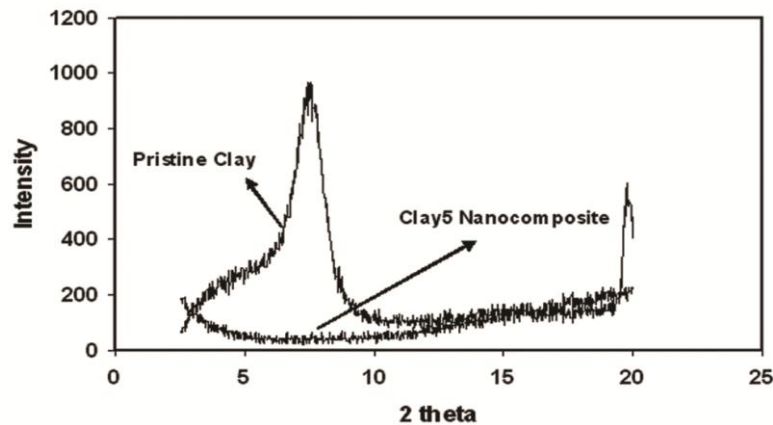


**Figure 1:** XRD patterns of pristine clay (a) and nanocomposite containing 5 wt% of nanoclay (b).

### 3.2. Dye adsorption studies

#### 3.2.1. Effect of clay content on the dye adsorption

The rate of dye adsorption of nanocomposites as a function of clay content is shown in Figure 3a. All samples were contacted with solutions containing  $50 \text{ mg L}^{-1}$  of MB and at the specified time intervals the adsorption capacity was recorded. As can be seen from the figure, the clay easily affects the rate of dye removal. In fact, dye adsorption speed enhanced as the clay content in the nanocomposite composition was increased. According to the data, while the removal efficiency is 99 and 92 % for Clay5 and Clay3, it is only 88 % for hydrogel without clay (Clay0). The increase in dye adsorption capacity and rate of adsorption of dye by introducing of Na-MMt can be attributed to: (a) by inclusion of the nanoclay Na-MMt into hydrogel, because of negative surface of clay, the negative charge density will be increased. The higher content of Na-MMt in the nanocomposite, the higher negative charges exist in the hydrogel [21] (b) according to SEM micrographs, as the Na-MMt was introduced into hydrogels, a relatively porous surface was obtained. The increase in porosity results in an enhancement in surface area of adsorbent and subsequently, the dye adsorption capacity will be enhanced (c) the water absorbency of samples was studied and indicated that an increase in water absorbency is observed as the Na-MMt introduced into hydrogels (Figure 3b). In fact, the increase in water absorbency causes an increase in volumes of samples. So, the surface area of the adsorbents is increased and results in an enhancement in the dye adsorption capacity of samples.

#### 3.2.2. Adsorption Kinetic

Studying of adsorption kinetics represents the pollutant adsorption rate, which dominates the time of adsorbate adsorption at the solid-liquid surface [22]. In fact, kinetic of adsorption is one of the most factors for finding the efficiency of adsorption. Pseudo-first-order and pseudo-second-order kinetic models were examined to obtain rate constant and equilibrium adsorption capacity for all samples. So, kinetic data were analyzed using the following equations [23]:

Pseudo-first-order 
$$\ln(q_e - q_t) = \ln q_e - k_1 t \quad (2)$$

where,  $q_e$  and  $q_t$  ( $\text{mg g}^{-1}$ ) are the amount of adsorbed dye on the nanocomposites at equilibrium and at time  $t$ , respectively.  $k_1$  ( $\text{min}^{-1}$ ) presents the rate constant of first-order adsorption.

Pseudo-second-order 
$$\frac{t}{q_t} = \frac{1}{k_2 q_e^2} + \frac{t}{q_e} \quad (3)$$

where,  $k_2$  ( $\text{g mg}^{-1} \text{ min}^{-1}$ ) is rate constant of second-order adsorption and  $q_e$  is the theoretical adsorbed dye ( $\text{mg g}^{-1}$ ) that can be calculated from pseudo-second-order.

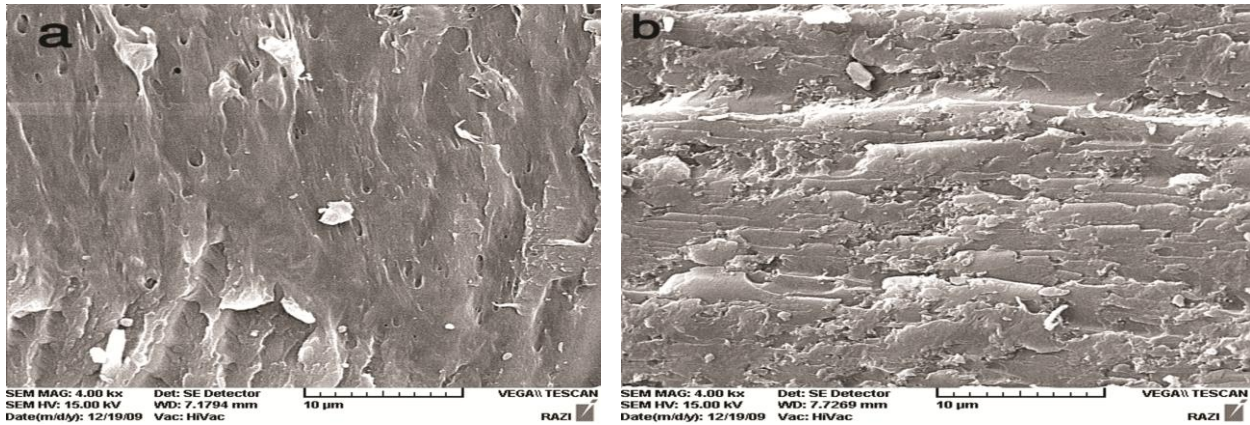


Figure 2: SEM micrographs of (a) clay-free hydrogel and (b) nanocomposite containing 5 wt% of nanoclay.

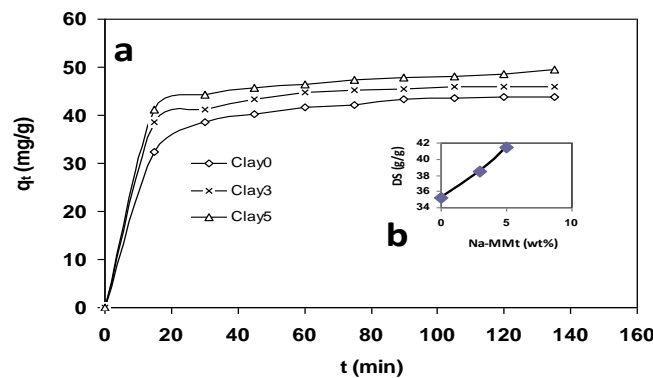


Figure 3: Effect of nanoclay content on (a) the dye adsorption speed of nanocomposites (b) degree of swelling of hydrogels.

In order to obtain model calculations, we can plot  $\ln(q_e - q_t)$  against  $t$  for pseudo-first-order and  $\frac{t}{q_t}$  against  $t$  for pseudo-second-order. For example, the curves for Clay5 nanocomposite were illustrated in Figure 4a and b.

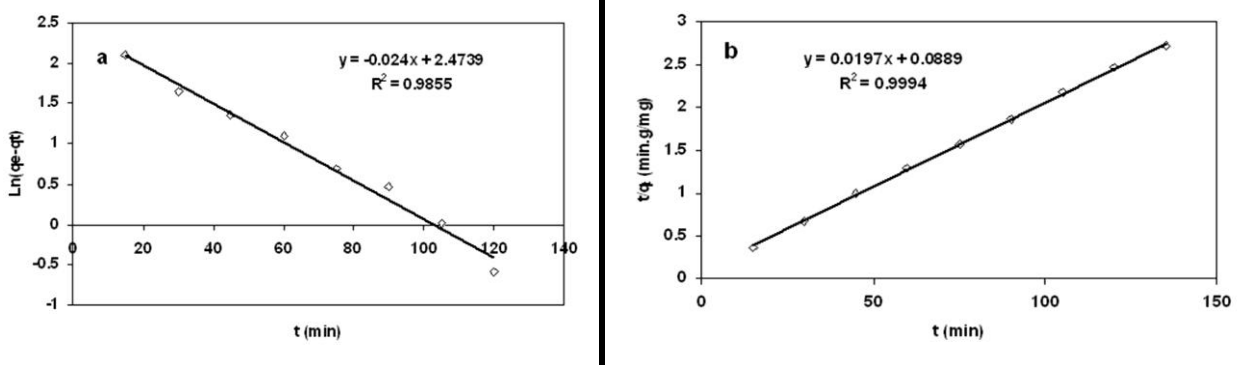


Figure 4: Adsorption kinetic of the MB onto Clay5 nanocomposite according to (a) pseudo-first-order and (b) pseudo-second-order models

Model calculations for all nanocomposites were given in Table 1. It was found that the plotting of  $\frac{t}{q_t}$  against  $t$

gives a straight-line with a high correlation coefficient ( $R^2 > 0.99$ ) and it can be concluded that adsorption kinetic of dye by all samples has the best fitting to the pseudo-second-order. As can be seen from the data, according to pseudo-second-order kinetic, the experimental and theoretical equilibrium adsorption capacities of nanocomposites are in agreement. Considering the  $k_2$  values, the adsorption rate constant of clay-free hydrogel is  $3.43 \times 10^{-3} \text{ g mg}^{-1} \text{ min}^{-1}$  and it increases for hydrogels including nanoclay component. This finding is consistent with experimental data of adsorption rates by varying nanoclay content.

The adsorption of adsorbate to the adsorbent can take place through several steps. The steps may be considered as film diffusion, pore diffusion, surface diffusion, and adsorption on the pore surface. In fact, under sufficient speed of stirring, intraparticle diffusion/transport process are the rate-limiting steps of adsorption kinetic [15]. The possibility of intra-particle diffusion can explore according to Eq. 4:

$$q_t = k_{id}t^{0.5} + C \quad (4)$$

Where  $q_t$  is the amount of dye adsorbed at time  $t$ ,  $C$  is the intercept and  $k_{id}$  is the intraparticle diffusion rate constant ( $\text{mg min}^{0.5}/\text{g}$ ).

**Table 1:** Kinetic parameters for adsorption of MB onto nanocomposites

	pseudo-first-order			pseudo-second-order			qe. Exp. (mg/g)
	$k_1$ ( $\text{min}^{-1}$ )	$q_{e1}$ , theo. (mg/g)	$r^2$	$k_2 \times 10^{-3}$ (g/mg.min)	$q_{e2}$ , theo. (mg/g)	$r^2$	
Clay0	0.0365	8.25	0.98	3.43	46.08	0.9999	43.94
Clay3	0.0413	13.7	0.95	5.7	47.3	0.9999	46.12
Clay5	0.024	7.8	0.98	4.36	50.7	0.9994	49.52

According to Eq. 4, by plotting  $q_t$  versus  $t^{0.5}$ , a straight line suggests that the intraparticle diffusion is the rate limiting step. As can be seen from Figure 5, the diffusion plot of MB onto nanocomposites is multi-linear containing two or three linear parts. The linear segments did not pass through the origin, indicating that the intraparticle diffusion is not the only rate limiting step. The first linear segments show that the mass transfer controlling may be due to boundary layer effect [24]. In order to determine exact mechanism of adsorption, experimental data analyzed according to Boyd's model [22]:

$$F = 1 - \frac{6}{\pi^2} \exp(-Bt) \quad (5)$$

Where  $F$  ( $F = \frac{q_t}{q_e}$ ) is the fractional attainment of equilibrium at different times,  $t$ , and  $Bt$  is a mathematical function of  $F$ .

The value of  $Bt$  can calculate according to Eq 6:

$$Bt = -0.4977 - \ln(1 - F) \quad (6)$$

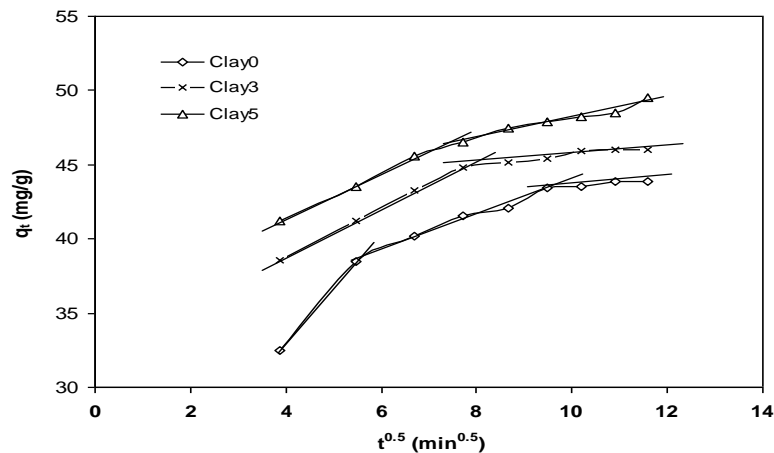


**Figure 5:** Intraparticle diffusion kinetics of MB dye onto nanocomposites.

The values of  $Bt$  can be calculated from  $F$  values at each time. The Boyd plot can be achieved by plotting of  $Bt$  versus  $t$ . A straight-line passing through the origin is indicative of sorption process governed by intraparticle diffusion mechanism. Non-linear plot shows that the adsorption dominates by film diffusion [24]. Figure 6 illustrates the plotting of  $Bt$  versus  $t$ . According to the Figure 6, the beginning of plot is straight linear and then deviates from origin. In can be concluded that the first time of adsorption obeys layer boundary effect and then the intraparticle diffusion dominates the mechanism of adsorption [24].

### 3.2.3. Adsorption Isotherms

The adsorption of MB onto nanocomposites as a function of initial dye concentration was studied by immersing 0.05 g of selected nanocomposites into dye solution with concentrations ranging from 10-1000  $\text{mg L}^{-1}$ . The results were indicated in Figure 7. Initially, as the concentration of MB in solution was increased, the amount of adsorbed dye by nanocomposites was increased and at high concentration of MB begun to level off. This indicates that the adsorbent gradually became saturated and approached a state of maximum adsorption. This observation can be attributed to the increase in momentum of the mass transfer as the initial dye concentration is increased [25]. In fact, when the nanocomposites are reached on a saturated state, there are no more vacant adsorption sites and the adsorption capacity remains constant.

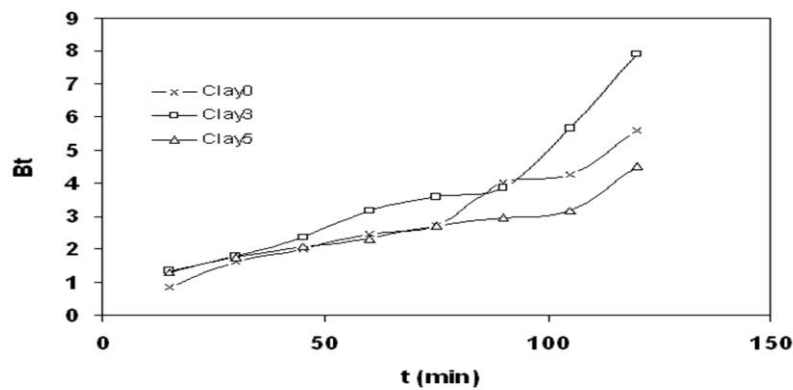


Figure 6: Boyd plot for sorption of MB dye onto nanocomposites.

The interactions between adsorbate and adsorbent until a state of equilibrium can be studied using adsorption isotherms. The adsorption isotherms describe the optimize adsorption system as well as the effectiveness of adsorbents [25]. In fact, it is important to investigate to obtain an optimum isotherm model indicating the MB adsorption system onto nanocomposite hydrogels. The practical data were fitted to the Langmuir and Freundlich models. In the Langmuir adsorption model, adsorption of adsorbate takes place at specific homogeneous sites within the adsorbent and valid for monolayer adsorption onto adsorbents. The expression of the applied Langmuir model is given by the Eq 7 [18]:

$$\frac{C_e}{q_e} = \frac{C_e}{q_m} + \frac{1}{q_m b} \quad (7)$$

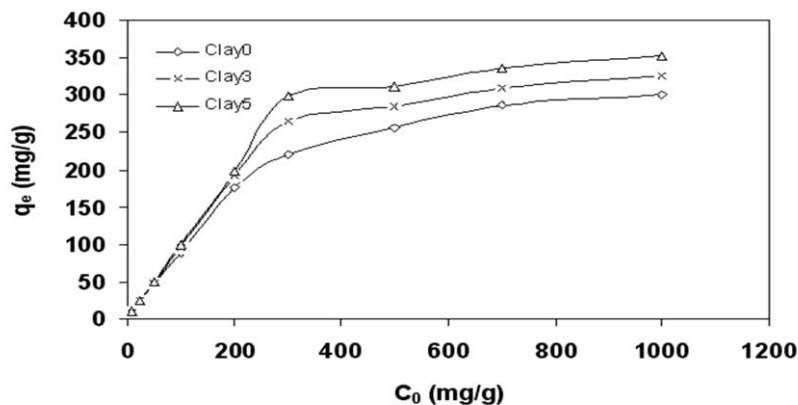


Figure 7: Effect of initial dye concentration on equilibrated adsorption capacity of nanocomposites.

In the Freundlich model, the adsorption of adsorbate occurs on a heterogeneous surface by multilayer sorption and the adsorption capacity can increase with an increase in adsorbate concentration [26]. Freundlich isotherm is represented by the following equation:

$$\text{Ln}q_e = \text{Ln}k_f + \frac{1}{n} \text{Ln}C_e \quad (8)$$

where,  $K_f$  is the equilibrium adsorption coefficient ( $\text{L g}^{-1}$ ), and  $1/n$  is the empirical constant. The  $K_f$  and  $n$  values for nanocomposites can be achieved from the intercept and the slop of plotting of  $\text{Ln}q_e$  against  $\text{Ln}C_e$ . The all expressions in Langmuir and Freundlich equations and equilibrated dye adsorption of all nanocomposites were calculated according to experimental data and summarized in Table 2.

Table 2: Parameters, correlation coefficient, and experimental  $q_m$  of nanocomposites according to Langmuir and Freundlich isotherms.

	Langmuir Model			Freundlich Model			$q_m, \text{exp.}$ (mg/g)
	$q_m, \text{mg/g}$	$b, \text{L/mg}$	$R^2$	$n, \text{g/L}$	$K_f, \text{mg/g}$	$R^2$	
Clay0	303	0.041	0.998	2.15	21.1	0.924	300.2
Clay3	322	0.095	0.998	2.47	35.72	0.849	325
Clay5	344	0.22	0.998	3.41	73.75	0.697	352.2

In accordance the high correlation coefficient in Langmuir equation ( $R^2 > 0.99$ ), it depicts that Langmuir isotherm is the best fit of experimental data than the Freundlich model. In addition, as can be seen from Langmuir data, the theoretical maximum adsorption capacity ( $q_m$ ) is in consistent with the experimental data. Considering the results, it is concluded that the adsorption of MB onto nanocomposites take places through mono layer adsorption.

### 3.2.4. Effect of particle size

In this section, we tried to investigate the effect of particle size of adsorbents on the adsorption of dye onto samples. Clay3 was chosen and the results are illustrated in Figure 8. As can be seen from figure, the removal efficiency of dye by adsorbent was enhanced from 86.4 to 99 % as the particle size was decreased from 400-840  $\mu\text{m}$  to 177-250  $\mu\text{m}$ . also, from the initial slope of the curves it is concluded that the rate of dye adsorption onto adsorbents was increased as the particle size was decreased. This can be attributed to this fact that for a given mass of adsorbent, the decrease in particle size can increase surface area availability and subsequently, the number of active sites for dye adsorption is increased [27].

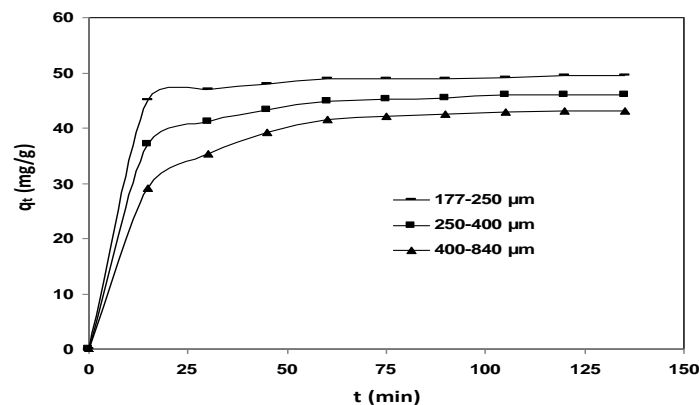


**Figure 8:** Effect of particle size of Clay3 adsorbent on dye adsorption capacity.

### 3.2.5. Thermodynamic Studies

The thermodynamic parameters of adsorption process were evaluated from examination of adsorption capacity of Clay3 nanocomposite at different temperature (297, 307, and 317 K). Adsorption enthalpy ( $\Delta H$ ,  $\text{kJ mol}^{-1}$ ), adsorption free energy ( $\Delta G$ ,  $\text{kJ mol}^{-1}$ ), and adsorption entropy ( $\Delta S$ ,  $\text{J K}^{-1} \text{mol}^{-1}$ ) can be calculated according to the following equations [28]:

$$K_D = \frac{V}{m} \left( \frac{C_0}{C_e} - 1 \right) \quad (9)$$

$$\Delta G = -RT \ln K_D \quad (10)$$

$$\ln K_D = \frac{\Delta S}{R} - \frac{\Delta H}{RT} \quad (11)$$

where,  $K_D$  is the equilibrium constant ( $\text{L g}^{-1}$ );  $C_0$  is the initial dye concentration ( $\text{mg L}^{-1}$ ) and  $C_e$  is the equilibrium concentration of dye ( $\text{mg L}^{-1}$ );  $R$  is the universal gas constant ( $8.314 \text{ J mol}^{-1} \text{ K}^{-1}$ ); and  $T$  is the absolute temperature (K). According to Eq. 11, by plotting the  $\ln K_D$  versus  $1/T$ , we can obtain the  $\Delta H$  and  $\Delta S$  from slope and intercept of linear plot, respectively (Figure 9).

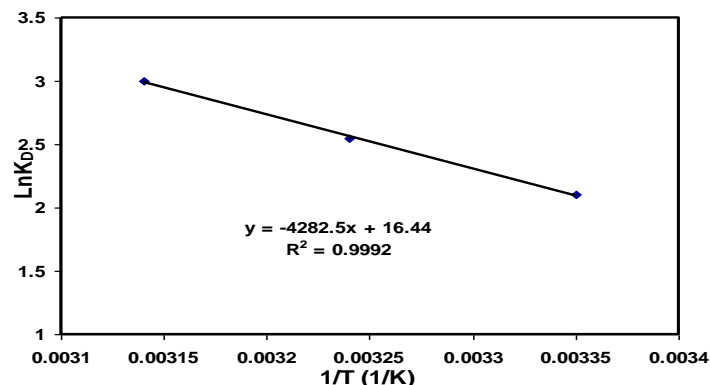


**Figure 9:** Plotting of  $\ln K_D$  versus  $1/T$  to obtain thermodynamic parameters (Clay3).

The results were summarized in Table 3. The negative values of  $\Delta G$  revealed that the adsorption of CV onto nanocomposites occurred spontaneously and the adsorption process of dye onto adsorbent was favourable at desired

temperatures. According to  $\Delta G$  values, the adsorption capacity of CV onto nanocomposite was increased and indicated that with increasing the temperature of dye solution, the favourability of CV adsorption onto nanocomposite is enhanced. Also, the positive value of  $\Delta S$  for the Clay3 nanocomposite suggests an increase in degree of freedom of the adsorbed species on the nanocomposite. The positive value of  $\Delta H$  showed that the adsorption of CV onto nanocomposite was endothermic.

**Table 3:** Thermodynamic parameters for adsorption of methylene blue onto Clay3. (Initial dye concentration: 50 mg/L, Adsorbent dosage: 50 mg, Volume of dye solution: 50 mL)

T (K)	$\Delta S, \text{J K}^{-1} \text{mol}^{-1}$	$\Delta H, \text{kJ mol}^{-1}$	$\Delta G, \text{kJ mol}^{-1}$	$R^2$
298	+136.7	+35.5	-5.2	0.9992
308			-6.5	
318			-7.9	

### Conclusion

Sodium

montmorillonite was introduced into carrageenan-based hydrogels. The obtained nanocomposites were applied for removing MB cationic dye from water. From the results obtained, the following conclusions can be drawn:

- According to XRD studies, the type of clay dispersion in nanocomposite matrix was exfoliated. The SEM micrographs showed that inclusion of Na-MMt can cause undulant surface.
- The obtained nanocomposites were examined to remove of MB dye from water. The results showed that the speed of dye removal can affect by clay content. The speed of dye removal was increased by introducing of nanoclay into hydrogel composition.
- The results showed that the pseudo-second-order adsorption kinetic was predominated for the adsorption of MB onto nanocomposite hydrogels.
- Langmuir model was obtained as the best model for the adsorption of MB onto nanocomposites.
- The decrease in particle size improved the rate of adsorption and content of adsorbed dye.
- Thermodynamic parameters revealed that the adsorption of MB onto adsorbent takes place spontaneously.

### References

1. Eshel, H., Dahan, L., Dotan, A., Dodiuk, H., Kenig, S., *Polym. Bull.* 61 (2008) 257.
2. Po, R., *J. Macromol. Sci. Rev. Macromol. Chem. Phys.* C34 (1994) 607.
3. Kost, J., In *Encyclopedia of Controlled Drug Delivery*, Mathiowitz E (Ed), Wiley, New York (1999).
4. Bulut, Y., Akcay, G., Elma, D., Serhatli, I.E., *J. Hazar. Mater.* 171 (2009) 717.
5. Hamidi, M., Azadi, A., Rafiei, P., *Adv. Drug Delivery Review* 60 (2008) 1638.
6. Jiuhui, Q., *J. Environ. Sci.* 20 (2008) 1.
7. Ahmad, R., Kumar, R., *Clean-Soil, Air, Water* 39 (2011) 74.
8. Sarri, M.M., *Water Sci. Technol.* 61 (2010) 2097.
9. Karadag, E., Saraydin, D., Guven, O., *J. Appl. Polym. Sci.* 61(1996) 2367.
10. Dutta, P.K., Dutta, J., Tripathi, V.S., *J. Sci. Ind. Res.* 63 (2004) 20.
11. Haraguchi, K., *Curr. Opin. Solid St. M.* 11 (2007) 47.
12. Liu, P., Zhang, L., *Sep. Purif. Technol.* 58 (2007) 32.
13. Dalaran, M., Emik, S., Guclu, G., Iyim, T. B., Ozgumus, S., *Polym. Bull.* 63 (2009) 159.
14. Li, P., Siddaramaiah, Kim, N.H., Yoo, G.H., Lee, J.H., *J. Appl. Polym. Sci.* 111 (2009) 1786.
15. Liu, Y., Wang, W., Jin, Y., Wang, A., *Sep. Purif. Technol.* 46 (2011) 858.
16. Ekici, S., Isikver, Y., Saraydin, D., *Polym. Bull.* 57 (2006) 231.
17. Abou-Taleba, M.F., Hegazy, D.E., Ismail, S.A., *Carbohydr. Polym.* 87 (2012) 2263.
18. Mahdavinia, G.R., Zhalebaghy, R., *J. Mater. Environ. Sci.* 3 (2012) 895.
19. Mahdavinia, G.R., Massoudi, A., Baghban, A., Massoumi, B., *Iran. Polym. J.* 21 (2012) 609.
20. Mahdavinia, G.R., Massoumi, B., Jalili, K., Kiani, G.R., *J. Polym. Res.* 19 (2012) 9947.
21. Abdel-Halim, E.S., Al-Deyab, S.S., *Carbohydr. Polym.* 86 (2011) 1306.
22. Tsai, W.T., Lai, C.W., Hsien, K.J., *J. Colloid Interface Sci.* 263 (2003) 29.
23. Kiani, G.R., Dostali, M., Rostami, A., Khataee, A.R., *Appl. Clay Sci.* 54 (2011) 34.
24. Li, A., Zhang, J., Wang, A., *J. Appl. Polym. Sci.* 103 (2007) 37.
25. Hameed, B.H., Din, A.T.M., Ahmad, A.L., *J. Hazar. Mater.* 141 (2007) 819.
26. Abdel-Halim, E.S., Al-Deyab, S.S., *Carbohydr. Polym.* 86 (2011)1306.
27. Ho, Y.S., Chiang T.H., Hsueh Y.M., *Process Biochem.* 40 (2005) 119.
28. Meroufel B., Benali O., Benyahia M., Benmoussa Y., Zenasni M.A., *J. Mater. Environ. Sci.* 4 (2013) 482.